ELSEVIER

Journal of Organometallic Chemistry 570 (1998) 89–96

Journal of Organometallic Chemistry

Solid-state and solution structures of several new $[LnCp'_2(OR)]_2$ complexes (Ln = Pr, Yb) with chiral, oxygen-functionalized μ-alkoxide ligands

Annette Steudel, Jens Stehr, Eric Siebel, R. Dieter Fischer *

Institut für Anorganische und Angewandte Chemie der Universität Hamburg, Martin-Luther-King-Platz 6, D-20146 Hamburg, Germany

Received 5 May 1998; received in revised form 12 June 1998

Abstract

Nine novel organolanthanoid (Ln = Pr and Yb) complexes of the general type $[LnCp'_2(\mu\text{-}OCHR^{(1)}Z)]_2$ ($Cp' = C_5H_5$ or $CH_3C_5H_4$, $R^{(1)} = H$ or Me) containing exclusively chiral, oxygen-functionalized alkoxide ligands with $Z^{(1)} = CHR^{(2)}OMe$ ($R^{(2)} =$ Me or Ph), $Z^{(2)} = COOi\text{Bu}$ and $Z^{(3)} = CH_2COOEt$ have been prepared and further characterized. While five (of six) Pr complexes give rise to solution ^{1}H-NMR spectra indicative of stable (on the NMR time scale) intramolecular coordination of Z via an additional O → Pr bond (as in form **B** of Fig. 1), the corresponding Yb-homologues turn out to be fluxional at room temperature. In contrast, X-ray diffraction studies of two new representatives with Ln = Yb, and of one selected complex with Ln = Pr, confirm the earlier suggested view (Steudel et al., J. Organomet. Chem. 556 (1998) 229) that in the solid state the central Ln(III) ion adopts the highest possible coordination number. © 1998 Elsevier Science S.A. All rights reserved.

Keywords: Lanthanide complexes; μ-Alkoxide; Ligands

---

1. Introduction

Owing to the pronounced, primarily kinetic weakness of metal-to-ligand bonds in (organo-) lanthanoid (Ln) compounds [1], complexes of the Ln elements tend to undergo in solution various kinds of (i.e. both intra- and intermolecular) facile ligand redistribution equilibria. Presently, the characterization of organo-Ln compounds is based predominantly on their crystallographic X-ray structures, i.e. on typical solid-state properties, although numerous organo-Ln systems may be considered as quite promising solution NMR candidates, too [2]. Organo-Ln compounds are often sufficiently soluble even in non-polar (i.e. chemically non-interfering) organic NMR solvents some of which remain liquid down to ca. − 80°C. Moreover, the *para*magnetism of several Ln(III) ions (e.g. Pr, Nd and Yb) offers in total more advantages than drawbacks in view of a successful observation and promising evaluation of their solution NMR spectra [3].

In the present contribution we continue reporting on novel insights into the solid-state and solution behavior of various dinuclear bis(cyclopentadienyl)lanthanoid(III)alkoxide systems. The generally metal-bridging alkoxide ligands of interest have, moreover, been either nitrogen [2] or oxygen-functionalized (Fig. 1). While crystallographic work has so far exclusively confirmed the presence of type **B** involving a rigid tricyclic skeleton [2,4–6], we have demonstrated more recently [2], in making use of suitable *para*magnetic NMR samples, that in solution the occurrence of species of type **A** cannot be excluded. In the following, the ^{1}H-NMR spectra of six Pr(III)- and four Yb(III)-complexes involving oxygen-functionalized alkoxide ligands will be examined in detail and compared with the molecular structures realized in three crystalline representatives of this series.

---

* Corresponding author. Tel.: + 49 40 41233100; fax: + 49 40 41232893.

0022-328X/98/$ - see front matter
PII S0022-328X(98)00802-X

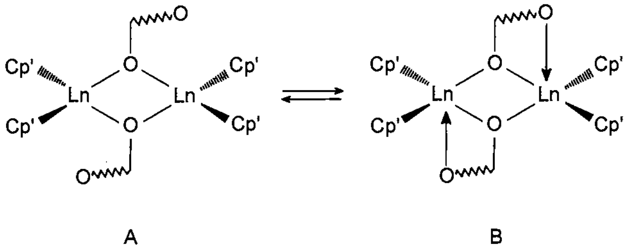

Fig. 1. Schematic view of the two structural alternatives **A** and **B** to be expected for all title complexes.

2. Preparation and general properties of the complexes 1–9

All title complexes were obtained in high yields in reacting at low temperature in toluene a selected tris(cyclopentadienyl)lanthanoid(III) system ($LnCp'_3$) with the corresponding oxygen-functionalized alcohol [2]. All alcohols (Scheme 1) were chiral and used as pure enantiomers to guarantee the observation of essential NMR spectroscopic features (vide infra). Moreover, in subsequent studies to be reported separately, the circular dichroism of selected f–f crystal field transitions of the Ln(III) ions was also investigated. While the alcohols H-EHB and H-IBL were commercially available, H-MOP and H-MPE had to be prepared from (L)-(−)-ethyllactate and (S)-(+)-mandelic acid, respectively. In particular, the enantioselective synthesis of H-MPE required well-controlled working conditions (see Section 6) to take care that the optical yield of this species did not become lower than 98.60%.

The essential building blocks of the strongly air-sensitive complexes **1**–**9** are, along with those of the already reported homologue **10** [5], listed in Table 1. All complexes are non-volatile in vacuo. Interestingly, ligand redistribution affording inter alia tris(cyclopentadienyl) metal complexes was not observed. Single crystals suitable for X-ray crystallography have so far been obtained for **4**, **7** and **9** from concentrated solutions in toluene.

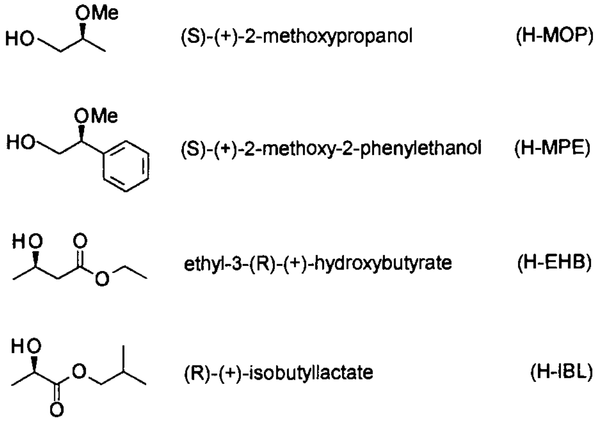

Scheme 1. Formulae, names and abbreviations of the four functionalized alcohols used as ligand precursors.

Table 1
Specification of the $[LnCp'_2Q]_2$ systems **1**–**10**

Number	Ln	η^5-Cp′	Alkoxide ligand (Q)[b]	Color
1	Pr	C_5H_5	MOP	Almost white
2	Pr	$CH_3C_5H_4$	MOP	Pale green
3	Pr	$CH_3C_5H_4$	MPE	Yellowish green
4[a]	Pr	C_5H_5	IBL	Pale green
5	Pr	$CH_3C_5H_4$	IBL	Pale green
6	Pr	$CH_3C_5H_4$	EHB	Pale green
7[a]	Yb	$CH_3C_5H_4$	MOP	Orange
8	Yb	C_5H_5	MPE	Bright yellow
9[a]	Yb	$CH_3C_5H_4$	MPE	Orange
10 [5][a]	Yb	C_5H_5	IBL	Yellow

[a] Subjected to a crystallographic X-ray study.

[b] For an explanation of the abbreviations below see Scheme 1.

3. Solid-state molecular structures of 4, 7 and 9

Crystal parameters of relevance for the X-ray studies of **4**, **7** and **9** are listed in Table 2. All three complexes crystallize, in accordance with the presence of (two) chirogenic centers, in the chiral space group $P2_1$, and the molecular structures (Figs. 2–4) correspond, in agreement with earlier findings [2,4–6], throughout to type **B** of Fig. 1. While **4** is almost isostructural with **10** [5], the structure of **7** resembles strongly that of **9** if the presence of two phenyl groups (in **9**) instead of two methyl groups (in **7**) is accounted for. Each of the four dinuclear complexes **4**, **7**, **9** and **10** consists of two $\{Cp'_2LnO^{(1)}O^{(2)}O^{(3)}\}$ units with three approximately ‘meridional’ [7] oxygen atoms next to the Ln(III) ion. Two O-atoms (O^b) belong to both Ln-atoms. Selected bond distances and angles, respectively, of **4**, **7**, **9** and **10** are listed in Table 3. For better comparison of corresponding data, several additional shorthands (see the bottom of Table 3) have been introduced. The perspective of the structure of **9** depicted in Fig. 4 indicates that even the methoxy carbon atoms (C9 and C18) lie in the Yb_2O_4 plane of the tricyclic skeleton of the complex. A corresponding situation is true for complex **7**. Actually, the three bond angles involving each of the ether oxygen atoms of **7** (O2 and O21) and **9** (O3 and O4) sum up to 355.5, 349.9, 356.1 and 349.5 degrees, respectively, suggesting that these oxygen atoms are near-sp^2-hybridized. Thus these ether oxygen atoms are not expected to function as additional chirogenic centers in close proximity to the metal ion.

Table 2
Crystal data and structure refinement parameters of **4**, **7** and **9**

	4[a]	**7**[b]	**9**[b]
Empirical formula	$C_{34}H_{46}O_6Pr_2$	$C_{32}H_{46}O_4Yb_2$	$C_{42}H_{50}O_4Yb_2$
Formula weight (g mol^{-1})	832.55	840.76	946.90
Temperature (K)	293(2)	153(2)	153(2)
Crystal system	Monoclinic	Monoclinic	Monoclinic
Space group	$P2_1$	$P2_1$	$P2_1$
a (pm)	873.0(2)	902.9(2)	913.5(7)
b (pm)	1910.3(4)	970.5(4)	1998.1(4)
c (pm)	1084.7(3)	1713.2(8)	1016.2(5)
β (°)	96.04(2)	94.58(3)	96.46(6)
V (10^6 pm^3)	1798.9(7)	1496.4(10)	1843.1(4)
Z	2	2	2
$D_{calc.}$ (g cm^{-3})	1.537	1.866	1.739
Diffractometer/wavelength	Synthex $P2_1$, Mo–K_α	Hilger and Watts Y290, Mo–K_α	Hilger and Watts Y290, Mo–K_α
Absorption coefficient (cm^{-1})	27.14	62.45	50.83
F(000)	832	820	948
Θ-Range (°)	$2.35<\Theta<25.06$	$2.26<\Theta<27.56$	$2.24<\Theta<27.46$
Index range	$-10\leq h\leq 10$, $-22\leq k\leq 22$, $-12\leq l\leq 12$	$-2\leq h\leq 11$, $-2\leq k\leq 12$, $-22\leq l\leq 22$	$-1\leq h\leq 11$, $-1\leq k\leq 25$, $-13\leq l\leq 13$
Reflections collected	9603	6011	5439
Independent reflections	6149	4474	4526
Absorption correction (DIFABS) T_{min}, T_{max}			0.165, 1.000
Data/restraints/parameters	6149/8/392	4474/1/356	4525/61/383
R indices (all data) (R_1, wR_2)	0.0608, 0.1291	0.0264, 0.0606	0.0527, 0.1071
Final R indices ($I>2$ s) (R_1, wR_2)	0.0479, 0.1191	0.0248, 0.0599	0.0441, 0.1019
Largest diff. peak and hole (e 10^{-6} pm^{-3})	1.008 and −1.654	2.215 and −1.346	1.776 and −2.750

[a] This crystal structure was solved using the SHELXTL-PLUS V4.2 software and revised with SHELXL-93.

[b] The structure was determined by using SHELXL-93.

According to a first systematic comparison of relevant structural data of **4**, **7**, **9** and **10** (Table 3) with corresponding values of earlier reported dinuclear $[Cp'_2Yb(\mu\text{-}OR)]_2$ systems devoid of a third meridional O-atom, both the Ln-O and Ln···Ln distances in the latter systems turn out to be significantly shorter (Table 4). Moreover, each of the dinuclear, chiral molecules **4**, **7**, **9** and **10** involves four crystallographically non-equivalent Cp′-ligands and lacks therefore any non-trivial (local) symmetry element. In contrast, the earlier reported, closely related complexes $[Yb(CH_3C_5H_4)_2\{\mu\text{-}OCH(CH_2)_3O\}]_2$ [4] and $[Nd(C_9H_7)_2\{\mu\text{-}OCH_2CH(CH_2)_3O\}]_2$ [6] which contain (per molecule) a racemic pair of the functionalized alkoxide ligand are, inter alia, centrosymmetric. However, in solution, each of the chiral molecules of type **B** would be likely to adopt, at least in average, a C_2 axis through its center of gravity (and perpendicular to the Ln_2O_2 plane), leaving no more than two non-equivalent Cp′-ligands [2].

The Ln–O distances involving an uncharged ether or carbonyl functionality are significantly longer than the (bridging) Ln–O^b distances. For instance, the two comparatively long Pr–O distances of **4** (253.0 and 255.5 pm) compare well with the Pr–O contact reported e.g. for $[Pr(C_5H_5)_3\cdot THF]$ (255.8 pm [10]), but exceed strongly the Pr–O distances of 240.5 and 241.3 pm involving the O^b-atoms of **4**. The longest Yb–O distances in **7** and **9** (245.6–251.3 pm) even exceed that found in $[Yb(C_5Me_5)_2Cl\cdot THF]$ (236.2 pm [11]), while the corresponding Yb–O^b contacts range only between 221.1 and 227.9 pm. The longest Yb–O distances in **9** exceed even that of $[Yb(C_5H_4Me)_2\{\mu\text{-}OCH(CH_2)_3O\}]_2$ (246.2 pm [4]). Thus the tricyclic configuration **B** of **9** might be rather labile and is likely to equilibrate in solution quite readily with configuration **A**.

4. Room temperature ^{1}H-NMR studies of 1–10

Making extensive use of the various criteria elaborated recently [2] during the evaluation of the NMR spectra of several complexes strongly related to **1**–**10**, although with nitrogen-functionalized, metal-bridging alkoxide ligands, the solution ^{1}H-NMR data collected in Table 5 may straightforwardly be interpreted as follows. All Pr-complexes except **3** should possess in solution two non-equivalent Cp′ ligands, owing to the appearance of either two separate C_5H_5 proton resonances, or of at least nine (ideal expectation: ten [2])

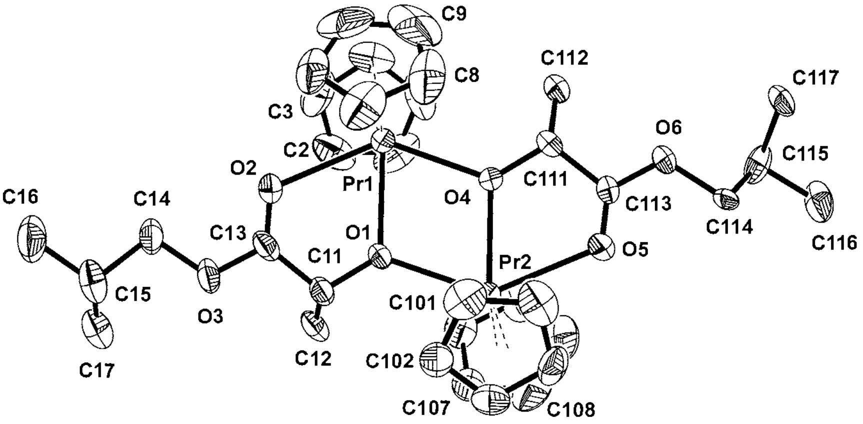

Fig. 2. ORTEP plot with atomic numbering scheme of complex **4**.

$CH_3C_5H_4$-resonances of the appropriate relative intensities. The latter findings can be rationalized in terms of two diastereotopic pairs of ring protons (for each of the two non-equivalent C_5H_4 units). This diastereotopic splitting is notably magnified by the paramagnetism of the Pr(III) ion. According to a preliminary variable-temperature (VT) ^{1}H-NMR study of **3**, the coalescence regime is passed below ca. 25°C, and exactly eight equally intense C_5H_4 proton singlets appear between 22 and 1 ppm. Likewise, two sharp CH_3 proton singlets are found between 6 and 1 ppm.

All these features are strongly in favor of substantial $Pr \leftarrow O$ bonding and consequently of the presence of the tricyclic isomer **B** (Fig. 1). In addition to the number of individual resonances, the magnitude of the isotropic shifts and of their separations confirm independently that also in solution the ether or carbonyl oxygen functionalities remain bonded to the Pr(III) ion. Dinuclear homologues of **1**, **2**, **5** and **6** with unfunctionalized alkoxide bridges have been shown [2] to display resonances located considerably more remote from the range spanned by the data of Table 5.

On the other hand, the Cp′ ring proton resonances of three of the four Yb-complexes investigated display either coalescence phenomena (**7** and in part **9**) or clear evidence of only one singular Cp′ ligand (**8**), suggesting that now the isomers **A** and **B** (Fig. 1) are rapidly equilibrating. Likewise, the room temperature ^{1}H-NMR spectra of the two homologues of **4** with Ln = Sm and Lu contain only one C_5H_5 proton resonance with $I_{rel} = 10$ ([5]b). Moreover, the Yb-complex **10** was shown to display at room temperature just one relatively broad C_5H_5 proton singlet, although below + 5°C clearly two well-separated resonances appear [5]. Evidently, the smaller ionic radius of Yb(III) relative to that of Pr(III) [14] makes all ytterbium complexes more reluctant to adopt the higher coordination number (of formally nine), via intramolecular chelation (according to Scheme 2). Interestingly, none of the three complexes involving the 2-phenyl-2-methoxy-ethanolate ligand (MPE, Table 1) seems to exist in solution exclusively as isomer **B**.

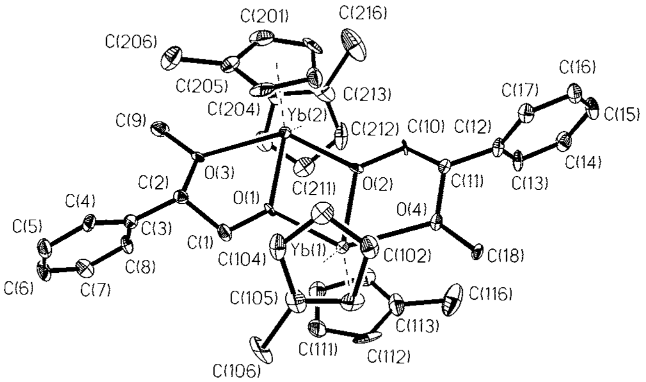

Fig. 3. ORTEP plot with atomic numbering scheme of complex **9** (view upon the Yb_2O_2 plane).

The proton resonances of the alkoxide ligands of **1**–**10** (for the notation of the various H atoms see Scheme 2) do not display any coalescence features. The positions of individual resonances are similar to those reported for several N-functionalized homologues [2]. The assignment of two distinct singlets to the α-CH_2 protons of the complexes **1**–**3** and **7**–**9** (Table 6) is tentatively based on a particular similarity in line width and relative intensity. Both the magnitude of the separation of these two signals, as well as of variations with the nature of the groups in the β- and γ-positions is surprising and might be due to the proximity of two paramagnetic Ln(III) ions. The δ-CH_2 protons of **4**, **5** and **10** experience genuine diastereotopic splitting of at least 0.46 (**5**) and maximally 2.3 ppm (**10**), while the ε-CH_2 protons of **6** give rise only to a common quartet at -3.39 ppm ($^3J = 5.7$ Hz). The adjacent CH_3 group contributes with a triplet at -3.42 ppm ($^3J = 5.6$ Hz). In contrast, the two methyl groups of **4**, **5** and **10** located beyond the δ-CH_2 group display weak, but significant diastereotopic splittings of 0.03 (Ln = Pr) to

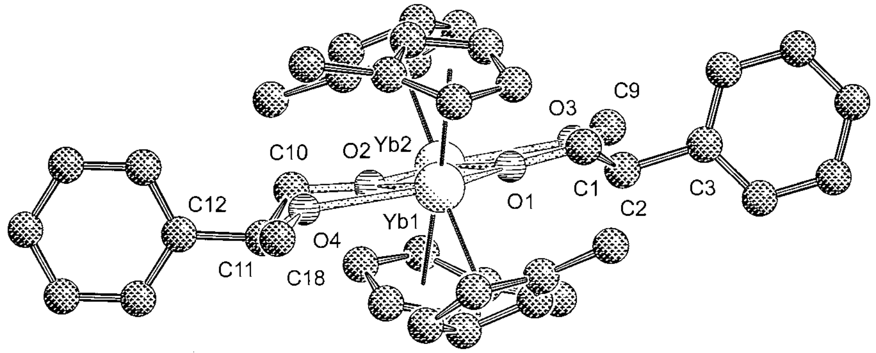

Fig. 4. Alternative perspective (parallel to the Yb_2O_2 plane) of the structure of **9** (SCHAKAL plot).

0.09 ppm (Ln = Yb). The methoxy protons of **1**–**3** and **7**–**9** always give rise to just one resonance with δ-values similar to those of the N-bonded methyl groups of corresponding complexes with nitrogen-functionalized alkoxide ligands [2]. This finding is in agreement with the crystallographic results (vide supra) according to which the formation of different stereoisomers is not very probable. According to the behavior of the C_5H_5 and $CH_3C_5H_4$ protons (vide supra), complex **10** seems to exhibit the highest coalescence temperature of all Yb-complexes studied. Accordingly, all proton resonances of the alkoxide ligands of **10** are more moderately displaced (towards lower fields) than the corresponding resonances of **7**, **8** and **9** (Table 6).

Table 3
Selected interatomic distances (pm) and bond angles (°) of **4**, **7**, **9**, and **10**

Distance/angle	**4** (Pr)	**7** (Yb)	**9** (Yb)	**10** (Yb) [5]
Ln1··Ln2	392.5(1)	373.5(18)	369.5(7)	369.5(1)
Ln1–O^{b1}	242.5(8)	223.3(5)	226.5(10)	226.9(8)
Ln1–O^{b2}	240.5(6)	228.0(6)	221.1(11)	230.1(5)
Ln2–O^{b1}	242.5(6)	227.7(6)	222.5(11)	228.0(6)
Ln2–O^{b2}	241.3(6)	222.7(5)	226.6(10)	223.8(9)
Ln1–O	255.5(8)	248.2(6)	251.3(12)	238.2(6)
Ln2–O′	253.0(8)	245.6(6)	247.6(12)	239.4(7)
Ln1–cent1	255.1(2)	241.1(2)	239.9(5)	238.3(5)
Ln1–cent2	252.7(2)	240.8(2)	239.8(5)	239.0(5)
Ln2–cent3	254.7(2)	239.9(2)	241.4(5)	238.3(4)
Ln2–cent4	253.5(2)	239.8(2)	239.2(5)	238.5(5)
O^{b1}–Ln1–O^{b2}	71.4(2)	68.0(2)	69.1(4)	70.7(3)
O^{b*}–Ln1–O′	65.6(2)	68.0(2)	67.8(4)	69.0(2)
cent1–Ln1–cent2	124.4(3)	123.3(3)	128.3(6)	125.5(3)
cent3–Ln2–cent4	126.1(3)	123.6(3)	127.1(4)	126.6(6)

O^{b1}, bridging oxygen atom with lowest number (according to the atomic numbering schemes in Figs. 2–4 and [5].
O and O′, respectively, corresponding non-bridging oxygen atom.
O^{b*}, the bridging oxygen atom generating an angle <90°.

5. Conclusions

The results of the present study complement and confirm our previous findings [2] according to which equilibria involving the two isomers **A** and **B** of heteroatom-functionalized, dinuclear bis(cyclopentadienyl)lanthanoid(III) alkoxides (Fig. 1) may efficiently be affected by (a) variation of the central metal ion Ln(III) (and hence of its ionic radius), (b) the nature of the additional heteroatom located on the bridging alkoxide ligand, and (c) the space demand of other organic groups belonging to the alkoxide and/or the cyclopentadienyl ligands. Thus larger (i.e. the 'earlier') Ln(III) ions favor strongly the preponderance of isomer **B** even in solution, and for a given Ln(III) ion NMe_2-functionalization is superior to OMe substitution. Ester functionalities turn out to coordinate via their carbonyl groups and appear to be even slightly more efficient than the NMe_2 group. The ν(CO) frequencies are lowered from the value of 1735 cm^{-1} for free H-EHB and H-IBL (Scheme 1) to values between 1680 and 1685 cm^{-1} in the cases of **4**–**6** and **10** [5]. Although the additional rings occurring in **B** involve five or six atoms, one example with only four ring atoms has also been reported [4].

Any rapid equilibrium $\mathbf{A} \rightleftharpoons \mathbf{B}$ should be accompanied by periodic elongations and shortenings of the Ln··Ln distance, which chemically induced 'breathing' phenomenon might deserve further attention.

6. Experimental section

All operations were carried out under a strict atmosphere of pure N_2, making use of familiar Schlenk techniques. Elemental analyses were carried out using the standard equipment applied for purely organic compounds. Consequently, the well-known difficulties arising for organolanthanoid complex are most probably reflected in some cases by unusually large deviations of the experimental values from the expected ones. IR spectra were obtained on a Perkin Elmer IR 1720

Table 4
Survey of Ln–O and Ln···Ln distances (in ppm) in earlier reported $[LnCp'_2(\mu\text{-}Q)]_2$ systems with two or three meridional oxygen atoms

Cp′	Ln	μ-Q	Ln–O^b		Ln–O^a	Ln··Ln	Ref.
C_5H_5	Yb	$O^b(CH_2)_4CH_3$	217(1)	219(1)	—	348.3(3)	[8]
C_5H_5	Yb	$O^bCMe{=}CHMe_2$	221.6(7)	220.3(5)	—	349.0(2)	[9]
C_5H_5	Yb	$O^b(CH_2)_2CHMe_2$	218.4(7)	221.0(6)	—	349.2(1)	[8]
C_5H_5	Yb	$O^bCH_2CH{=}CHMe$	219.6(7)	222(1)	—	352.3(2)	[4]
C_5H_4Me	Yb	$O^bCH(CH_2)_3O$	224.2(5)	228.2(5)	246.2(2)	372.2(7)	[4]
$C_5H_3(SiMe_3)_2$	Y	O^bMe	221.7(3)	223.3(3)	—	356.2(1)	[12]
C_9H_7	Nd	$O^bCH_2CH(CH_2)_3O$	230(1)	231(1)	251(1)	387(2)	[6]
$C_5H_4(tBu)$	Ce	$O^{b\,i}Pr$	236.9(3)	237.3(3)	—	384.4(2)	[13]

O^a: uncharged, non-bridging oxygen atom. O^b: bridging (alkoxide) oxygen atom.

Table 5
Room temperature ^{1}H-NMR data (chemical shifts in ppm) of the C_5H_5 or $CH_3C_5H_4$ protons of the complexes **1**–**10**

Sample/Ln	CH_3-resonances		C_5H_5/C_5H_4-resonances			
1 Pr	—		8.84 (5H)[a]			3.74 (5H)[a]
2 Pr	3.60 (6H)[b]	17.84 (1H)	12.28 (1H)	6.34 (1H)		ca. 3.9 (1H)[b]
		15.32 (1H)	11.70 (1H)	6.01 (1H)		1.62 (1H)
3 Pr			Near-coalescence between ca. 1 and 21 ppm			
4 Pr	—		7.48 (5H)[c]			4.77 (5H)[c]
5 Pr	2.89 (3H)	14.24 (1H)	11.90 (1H)	7.71 (1H)		4.54 (1H)
	1.65 (3H)	12.53 (1H)	10.62 (1H)	7.32 (1H)		−2.49 (1H)
6 Pr	9.08 (3H)	23.12 (1H)	6.78 (1H)	−2.99 (2H)		−4.95 (1H)
	8.64 (3H)	10.42 (1H)	1.26 (1H)			−11.89 (1H)
7 Yb			Coalescence between +10 and −40 ppm			
8 Yb	—			−30.70 (10H)		
9 Yb	Coalescence		−4.2 (4H)			−33.8 (4H)
10 Yb [5]	—			−12.24 (10H)[d]		

Solvent: CD_2Cl_2. At 10°C two singlets: −12.90 ppm (5H), and −17.70 ppm (5H).

[a] $\Delta_{1/2}$ = ca. 30 Hz.

[b] One broad singlet.

[c] $\Delta_{1/2}$ = ca. 50 Hz.

[d] $\Delta_{1/2} \approx 350$ Hz.

instrument, and mass spectra on a Varian 311 A spectrometer equipped with a Finnigan Spectro System MAT 188 data processor. All ^{1}H-NMR spectra were run at room temperature on either of the instruments: Bruker WP 80 (80 MHz), Varian Gemini 200 (200 HMz) and Bruker AM 360 (360 HMz), respectively (solvent: CD_2Cl_2). THF-free tris(cyclopentadienyl)lanthanoid(III) complexes, [LnCp‘$_3$] as well as their 1:1 THF-adducts were prepared according to the literature [15]. Ethyl-3-(R)-(+)-hydroxybutyrate (H-EHB) and (R)-(+)-isobutyllactate (H-IBL) were purchased from Fluka and Aldrich, while the other two functionalized alcohols of Scheme 1 were prepared as follows.

6.1. Preparation of (S)-(+)-2-methoxypropanol (H-MOP)

Following Purdie and Irvine [16], (L)-(−)-ethyllactate (Merck) and methyliodide were reacted under a strict N_2-atmosphere with silver(I)oxide to afford (S)-(+)-2-methoxy-ethyl-propionate (b.p.$_{20}$, 50°C; yield, 67%). Following Buchwald et al. [17] the latter was reduced with $LiAlH_4$ and subsequently reacted with $NaOH/H_2O$. After drying over $MgSO_4$, solvent evaporation in vacuo and fractionated distillation over a 16 cm Vigreux column at 90 torr, pure H-MOP was obtained as a colorless oil (yield, 70%). b.p.$_{90}$ = 74%; $[\alpha]_D^{20} = +21.6°$ (c = 0.45, $CHCl_3$). Literature [18]: + 19.6° (c = 0.47, $CHCl_3$). ^{1}H-NMR (360 MHz, $CDCl_3$): 3.57 m (2H) CH_2; 3.36 m (1H) CH; 3.39 s (3H) OCH_3; 3.14 bs (1H) OH; 1.13 d (3H, $^3J = 11.6$ Hz) CH_3.

6.2. Preparation of (S)-(+)-2 methoxy-2-phenylethanol (H-MPE)

Following Rose and Dräger [19], (S)-(+)-mandelic acid (98%, Fluka) was converted into (S)-(+)-2-methoxy-2-phenylacetic acid (yield: 6 g, 22%). $[\alpha]_D^{20}$: + 141.2° (c = 1.03, EtOH); literature [16]: + 143.2° (c = 1.0, EtOH). Subsequently, this intermediate was reduced with $LiAlH_4$. Pure H-MPE was finally ob-

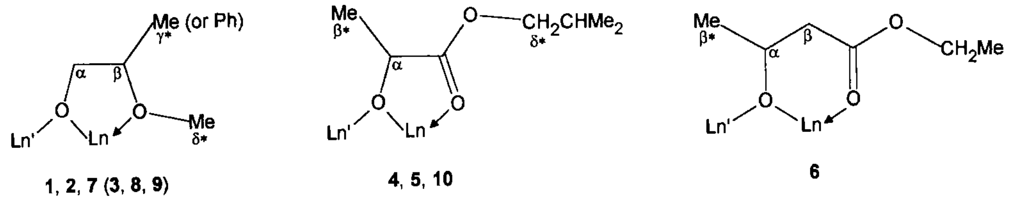

1, 2, 7 (3, 8, 9) 4, 5, 10 6

Scheme 2. Survey of the composition of the five- and six-membered rings resulting from intramolecular chelation.

Table 6
Room temperature ^{1}H-NMR data of the functionalized alkoxide ligands (δ in ppm) of the complexes **1**–**10**

Sample/Ln	α- and β-positioned protons				γ- and δ-positioned protons			
1 Pr	0.71 (1H)^{a}	−15.77 (1H)^{a}	−16.47 (1H)		−17.60 (3H)*		−21.48 (3H)*	
2 Pr	12.8 (1H)^{a}	−17.0 (1H)^{a}	−22.6 (1H)		−19.50 (3H)*		−22.90 (3H)*	
3 Pr	−6.43 (1H)^{a}	−33.30 (1H)^{a}	−33.63 (1H)		—		−28.95 (3H)*	
4 Pr	−9.64 (1H)^{a}		−16.24 (3H)*		—	−6.74 (1H)*^{b}		−7.60 (1H)*^{b}
5 Pr	−12.10 (1H)^{a}		−18.30 (3H)*		—	−8.91 (1H)*^{b}		−9.37 (1H)*^{b}
6 Pr	−3.49 (3H)*	−13.93 (1H)^{b,c}	−28.47 (1H)^{b,c}	−29.74 (1H)^{a}	—			
7 Yb	113.72 (1H)^{a}	85.30 (1H)^{a}	81.47 (1H)		47.52 (3H)*		76.47 (3H)*	
8 Yb	132.34 (1H)^{a}	98.51 (1H)^{a}	70.0 (1H)		—		80.86 (3H)*	
9 Yb	153.87 (1H)^{a}	99.47 (1H)^{a}	89.44 (1H)		—		88.21 (3H)*	
10^{e} Yb		43.01 (1H)^{a}	48.50 (3H)*		—	27.53 (1H)*		29.85 (1H)*

Data with an asterisk refer to exocyclic protons (based on the structures given in Scheme 2).

[a] Assumed to be α-protons.

[b] Doublet.

[c] Doublet ($^{2}J \approx 15.2$ Hz),

[d] Quartet ($^{3}J = 5.7$ Hz).

[e] Measurement at 10°C.

tained in a yield of 56%. $[\alpha]_{D}^{20}$: + 119° (c = 2.58, EtOH); literature [16]: 126° (c = 2.57, EtOH); optical yield p = 94.44%. ^{1}H-NMR (360 MHz, $CDCl_3$): 7.36 m (5H) C_6H_5; 4.31 dd (1H), $^{3}J = 3.6$ Hz) CH; 3.65 m (2H) CH_2; 3.31 s (3H) OCH_3; 2.48 bs (1H) OH.

The lanthanoid complexes **1**–**3** and **7**–**9** (Table 1) were prepared according to the representative description given in [2], while further instructions for the preparation of **4**–**6** may be found in [5]a; e.g. **3**: Prepared from 534.4 mg (1.41 mmol) of $[Pr(CH_3C_5H_4)_3]$ and 1.1 ml (214.5 mg; 1.41 mmol) of H-MPE (from a well-defined solution in toluene) using 75 ml of toluene in total. Reaction temperature: − 65°C. Yield: 603.2 mg (95%) of a microcrystalline, faintly green solid. Elemental analysis $C_{21}H_{25}O_2Pr$ calcd. C 56.01, H 5.60; found C 55.26, H 5.58%. **4**: Prepared from 815 mg (2.4 mmol) of $[Pr(C_5H_5)_3]$ and 0.36 ml (350 mg, 2.4 mmol) of H-IBL in 120 + 10 ml of toluene. Temperature: − 70°C. Yield: 906 mg (90.7%) of a faintly green microcrystalline solid. Elemental analysis $C_{17}H_{23}O_3Pr$ calcd. C 49.05, H 5.57; found C 48.51, H 5.52%. Decomp. temp. 180°C; IR, ν(CO) 1681 cm^{-1}. **6**: Prepared from 606 mg (1.60 mmol) of $[Pr(CH_3C_5H_4)_3]$ and 0.21 ml (212 mg, 1.60 mmol) of H-EHP in 50 ml of toluene (in total). Temperature: − 70°C, yield: 647 mg (93%) of a faintly green solid. Elemental analysis $C_{18}H_{25}O_3Pr$ calcd. C 48.81, H 6.02; found C 48.40, H 5.81%. IR, ν(CO) 1677 cm^{-1}. **9**: Prepared from 688.4 mg (1.7 mmol) of $[Yb(CH_3C_5H_4)_3]$ and 1.33 ml (258.7 mg, 1.33 mmol) of H-MPE in 75 ml of toluene (total) at − 60°C. Yield: 590.3 mg (92.0%) of an orange solid. Elemental analysis $C_{21}H_{25}O_2Yb$ calcd. C 52.28, H 5.22; found C 51.67, H 5.26%.

*6.3. X-ray crystallography (of **4**, **7** and **9**)*

Single crystals were grown from concentrated solutions of the complexes in toluene. The room temperature study of **4** was a compromise owing to limited availability of low-temperature instrumentation. The determination of the lattice parameters and the subsequent measurement of intensity data was based on the Θ/2Θ scan technique also taking care of the Friedel pairs of the throughout chiral molecules. Heavy atoms were located by three-dimensional Patterson synthesis, and subsequent difference Fourier and least-squares calculations have led to the positions of the C- and O-atoms. Phenyl and cyclopentadienyl rings were refined as rigid bodies with fixed C–C distances of 139 and 142 pm, respectively. For refinements including the H-atoms, the C–H distances were fixed to 96 pm. All non-hydrogen atoms were refined anisotropically [20].

Absolute configurations of the chiral ligand sites were controlled by inspection of anomalous dispersion effects [21].

Acknowledgements

Financial support by the BMBF, Bonn (Project Nr. 03D0023B/8) is gratefully acknowledged. We also thank S. Samba for technical assistance and Professor U. Behrens (Hamburg) for his continuous help in overcoming particular crystallographic problems.

References

[1] See: (a) G.R. Choppin, in: J.-C.G. Bünzli, G.R. Choppin (Eds.), Lanthanide Probes in Life, Chemical and Earth Sciences, Elsevier, Amsterdam, 1989, p. 1. (b) R.A. Anwander, W.A. Herrmann, in: W.A. Herrmann (Ed.), Topics in Current Chemistry, vol. 178, Springer, Berlin, 1996, p. 1, and further references given therein.

[2] A Steudel, E. Siebel, R.D. Fischer, G. Paolucci, V. Lucchini, J. Organomet. Chem. 556 (1998) 229 (and further references given therein).

[3] See (a) G.N. LaMar, W. DeW. Horrocks, Jr., R.H. Holm (Eds.), NMR of Paramagnetic Molecules, Academic Press, New York, 1971. (b) R.D. Fischer, in: T.J. Marks, R.D. Fischer (Eds.), Organometallics of the f-Elements, D. Reidel, Dordrecht, 1979, p. 337, and further references cited therein. (c) W. Jahn, K. Yünlü, W. Oroschin, H.-D. Amberger, R.D. Fischer, Inorg. Chim. Acta 95 (1984) 85. (d) I. Bertini, C. Luchinat, NMR of Paramagnetic Molecules in Biological Systems, Benjamin-Cummings, Menlo Park, 1986.

[4] G. Massarweh, R.D. Fischer, J. Organomet. Chem. 444 (1993) 67.

[5] (a) J. Stehr, R.D. Fischer, J. Organomet. Chem. 459 (1993) 79. (b) J. Stehr, Dissertation, Universität Hamburg, Germany, 1993.

[6] W.-W. Ma, Z.-Z. Wu, R.-F. Cai, Z.-E. Huang, J. Sun, Polyhedron 16 (1997) 3723.

[7] Approximately, each oxygen triple lies within the mirror plane that would transform either of the two Cp′-ring normals into each other.

[8] Z.-Z. Wu, Z.-E. Huang, R.F. Cai, Z. Xu, X.-Z. You, X.-Y. Huang, Polyhedron 15 (1996) 13.

[9] Z. Wu, Z. Xu, X. You, X. Zhou, Y. Ying, Z. Jin, J. Organomet. Chem. 483 (1994) 107.

[10] Y. Fan, P. Lü, Z. Jin, W. Chen, Scientia Sinica Ser. B 27 (1984) 993.

[11] H. Yasuda, H. Yamamoto, K. Yokota, A. Nakamura, Chem. Lett. (1989) 1309.

[12] W.J. Evans, M.S. Sollberger, J.L. Shreeve, J.M. Olofson, J.H. Hain, J.W. Ziller Jr., Inorg. Chem. 31 (1992) 2492.

[13] S.D. Stults, R.A. Andersen, A. Zalkin, Organometallics 9 (1990) 1623.

[14] R.D. Shannon, Acta Crystallogr. A 32 (1976) 751.

[15] W.A. Herrmann, F.T. Edelmann (Eds.), Synthetic Methods of Organometallic and Inorganic Chemistry, vol. 6, Thieme, Stuttgart, 1997, p. 68.

[16] (a) T. Purdie, J.C. Irvine, J. Chem. Soc. 75 (1898) 483. (b) M.M. El-Abadelah, Tetrahedron 29 (1973) 589.

[17] S. Buchwald, D. Pliwa, J. Knowles, J. Am. Chem. Soc. 106 (1984) 4917.

[18] K. Yamamoto, Y. Nakao, Y. Kyogoku, H. Sugeta, J. Mol. Struct. 242 (1991) 75.

[19] U. Rose, M. Dräger, J. Med. Chem. 35 (1992) 2238.

[20] Full details of the crystal structure determination of **4**, **7** and **9** have been deposited at the Fachinformationszentrum Karlsruhe GmbH, D-76344 Eggenstein-Leopoldshafen, Germany, and can be obtained on quoting the depository numbers CSD 408600, 406284 and 406282, respectively.

[21] (a) J. Ibers, W.C. Hamilton, Acta Crystallogr. 17 (1964) 781. (b) H.D. Flack, Acta Crystallogr. A39 (1983) 876.